Wavelength-shifting fiber readout of $LaCl_3$ and $LaBr_3$ scintillators

Gary L. Case[a,b], Michael L. Cherry[b], J. Gregory Stacy[a,b], and Christopher E. Welch[b]

[a]Dept. of Physics, Southern University, Baton Rouge, LA 70813
[b]Dept. of Physics & Astronomy, Louisiana State University, Baton Rouge, LA 70803

ABSTRACT

Inorganic scintillators such as NaI(Tl) and CsI(Na) have been used extensively in hard x-ray and low-energy gamma-ray imaging systems. Recently, a new generation of scintillators has been developed with properties that could greatly enhance the performance of such imaging systems. In particular, the lanthanum halides show great promise with increased light yield and peak emission at shorter wavelengths compared to NaI or CsI. Since these scintillators emit at relatively short wavelengths, wavelength-shifting fibers can be used which re-emit at wavelengths around 420 nm, providing a good match to bialkali photocathode response. Multi-anode photomultiplier tubes can be used to read out individual fibers from orthogonal layers to provide x-y position information, while energy measurements can be made by large area photomultiplier tubes. Such an arrangement potentially provides improved overall position and energy resolution and lower thresholds compared to imaging systems configured as standard NaI or CsI gamma cameras. We present measurements of the energy resolution obtained from lanthanum chloride ($LaCl_3$) and lanthanum bromide ($LaBr_3$) scintillators viewed both perpendicular to the axis and down the length of square multi-clad wavelength-shifting fibers. These results are compared to a standard NaI detector with wavelength-shifting fibers. The implications of these results for gamma-ray imaging will then be discussed.

Keywords: gamma-rays, scintillators, lanthanum chloride, lanthanum bromide, wavelength shifting fibers, gamma-ray imaging

1. INTRODUCTION

Hard x-ray and gamma-ray imaging systems with large-area detector planes have found increasing use in fields such as medical imaging, nondestructive testing, monitoring for national security, and astronomy. The high energies of the photons to be detected necessitate the use of relatively thick, dense detector materials. Room temperature solid-state semiconductors such as cadmium zinc telluride (CZT) offer excellent energy and spatial resolution. However, cost and complexity issues currently make the development of large area CZT detectors extremely difficult. Inorganic scintillators, e.g. NaI(Tl) or CsI(Tl), provide a more affordable alternative along with the capability of being manufactured with large areas and thicknesses. These scintillators provide good timing and spatial resolution, although the energy resolution cannot match that of CZT. Pixellated scintillator detectors can potentially improve the spatial resolution, although the energy resolution remains poorer than that of CZT.

Recently, two new inorganic scintillators, cerium-doped lanthanum chloride ($LaCl_3$) and lanthanum bromide ($LaBr_3$), have been developed[1,2] with performance approaching that of semiconductors. These scintillators have slightly higher densities, significantly higher light output, shorter decay times, and shorter peak emission wavelengths than thallium-activated NaI or sodium-activated CsI (Table 1). The higher light output and shorter emission wavelength combine to give significantly better energy resolution when measured with a standard bialkali photomultiplier tube (PMT). When coupled to a wavelength-shifting (WLS) fiber whose absorption spectrum is matched to the scintillator emission, imaging systems can be constructed with performance that significantly exceeds that attainable with standard NaI or CsI based systems.

A WLS fiber imaging system (Figure 1) employs a scintillator plate with optical windows on both of the large faces. The windows are generally thin glass windows, as the scintillators considered here (with the exception

Send correspondence to: case@phunds.phys.lsu.edu

UV, X-Ray, and Gamma-Ray Space Instrumentation for Astronomy XIV
edited by Oswald H. W. Siegmund, Proceedings of SPIE Vol. 5898
58980K, (2005) · 0277-786X/05/$15 · doi: 10.1117/12.617796

Table 1. Characteristics of scintillator crystals.

Material	Density (g/cm^3)	Decay time (ns)	Peak emission wavelength (nm)	Light yield (photons/keV)
NaI(Tl)	3.7	250	415	38
CsI(Na)	4.5	630	420	41
CsI(Tl)	4.5	1000	550	54
$LaCl_3$	3.8	28	350	49
$LaBr_3$	5.3	26	380	63

of CsI(Tl)) are hygroscopic and must be hermetically sealed. A layer of fibers (x-fibers) is laid out along and optically coupled to the top window. Then another layer (y-fibers) is laid out orthogonal to the first layer and coupled to the bottom window. When a photon interacts in the crystal, the optical light produced is emitted isotropically, with half the light emitted in the upward direction, the other half downward. Those optical photons which are transmitted through the window are absorbed by the WLS fiber with essentially 100% efficiency. The WLS fiber then re-emits the light at a longer wavelength. A fraction of the re-emitted light ($\sim 15\%$ for a multi-clad square fiber with indices of refraction for the core, inner cladding and outer cladding of 1.60, 1.49 and 1.42, respectively[3]) is optically trapped in the fiber. Half of these photons propagate directly down the length of the fiber to the PMT. The opposite end of the fiber can either be read out with another PMT or covered with a reflective material (e.g., aluminum foil) to reflect the photons emitted in this direction back to the single PMT. Reflecting the light back to the PMT increases the light output of the fibers and effectively lowers the energy threshold.

If the individual WLS fibers are read out separately, e.g. mated to a multi-anode PMT, then the distribution of pulse heights in the x- and y-directions can be used to find the "pixel" where the interaction takes place. The energy measurement is made by coupling a large PMT (or an array of large PMTs) to the bottom layer of fibers via a light guide. The $\sim 85\%$ of re-emitted light that is not trapped by the WLS fibers will either exit through the bottom layer of fibers directly or exit after being reflected from a reflective layer placed above the top layer of fibers.

In order to optimize the energy resolution, position resolution, and minimum energy threshold of the system,

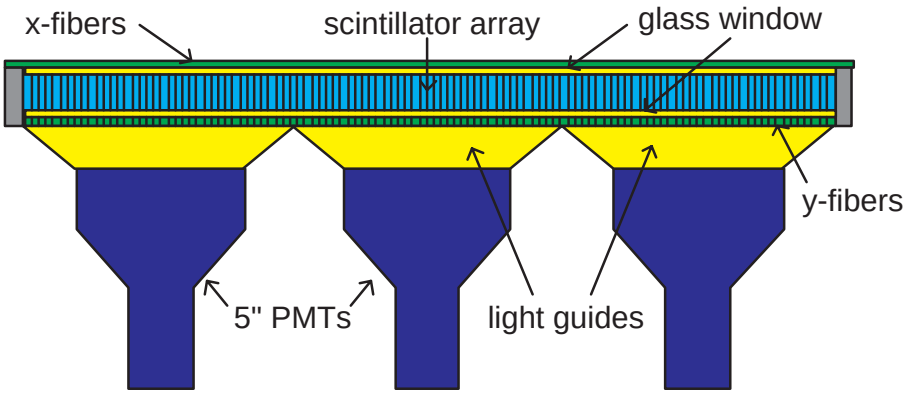

Figure 1. Fiber imaging system consisting of scintillator (in this case a segmented array of CsI(Na) consisting of optically isolated 2 x 2 mm^2 pixels) read out by crossed wavelength-shifting fibers and multi-anode PMTs (not shown). The fibers are used for position determination. The large area PMTs are used to measure the total energy deposit.

Table 2. Characteristics of wavelength-shifting fibers.

Fiber	Absorption peak (nm)	Emission peak (nm)	Scintillator
BCF99-90	345	435	$LaCl_3$
BCF99-33A	375	430	$LaBr_3$
BCF91A	420	494	NaI(Tl), CsI(Na)

the absorption spectrum of the WLS fibers must match the emission spectrum of the scintillator. The energy resolution is further maximized if the emission spectrum of the WLS fiber peaks at relatively short wavelengths where the quantum efficiency of the PMT photocathode approaches its maximum, and is narrow enough to minimize self-absorption. Table 2 lists WLS fibers manufactured by St. Gobain Crystals and Detectors appropriate for use with the scintillators under study here along with some of their relevant characteristics. The peaks of the emission spectra of both BCF99-90 and BCF99-33A are well matched to the quantum efficiency of a standard bialkalai photocathode, while the emission spectrum for the BCF91A peaks in a region where the quantum efficiency is somewhat lower.

In this paper, we will present the results of tests using $LaCl_3$ and $LaBr_3$ scintillators coupled to WLS fibers, including measurements of energy resolution perpendicular to the fiber axis and minimum energy threshold attainable from the fibers end-on. These results will be compared to a NaI detector also read out with WLS fibers with the same geometry. The implications of these results for gamma-ray imaging will then be discussed.

2. EXPERIMENTAL SETUP

Measurements were made using a $LaCl_3$ and a $LaBr_3$ detector provided by St. Gobain, both of which were 1" in diameter by 1" thick. Since both crystals are hygroscopic, they were each supplied in a hermetically-sealed thin aluminum can with a glass window on one end. Energy resolution measurements were first made by coupling each detector directly to a 2" Electron Tubes 9266 PMT with a standard bialkali photocathode using BC-630 optical grease. A NaI(Tl) detector, also 1" in diameter by 1" thick from St. Gobain, was used for comparison.

Appropriate WLS fibers were then coupled to the detectors (Table 2). For the NaI detector, the fibers used were manufactured by Washington University with the same dimensions and spectral properties as the BCF91A fibers. Figure 2 shows the experimental setup, which was identical for all three detectors. All WLS fibers were 2 mm $\times$ 2 mm $\times$ 50 cm square multi-clad fibers. For each detector, twelve fibers were laid out side-by-side and optically coupled to the glass window using optical grease. A 2" Electron Tubes 9266 PMT (the "energy PMT") was air-coupled to the fibers opposite the detector. The fibers were read out using another 2" Electron Tubes 9266 PMT (the "fiber PMT") which integrated the light out of the individual fibers. Aluminum foil was

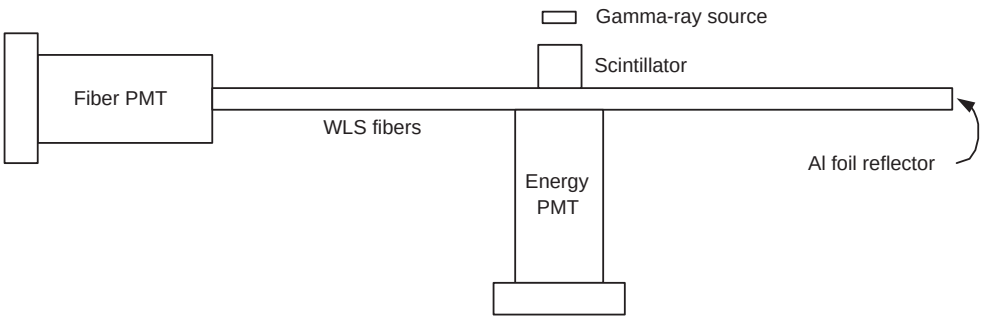

Figure 2. Experimental setup for $LaCl_3$ and $LaBr_3$ tests with wavelength-shifting fiber readout.

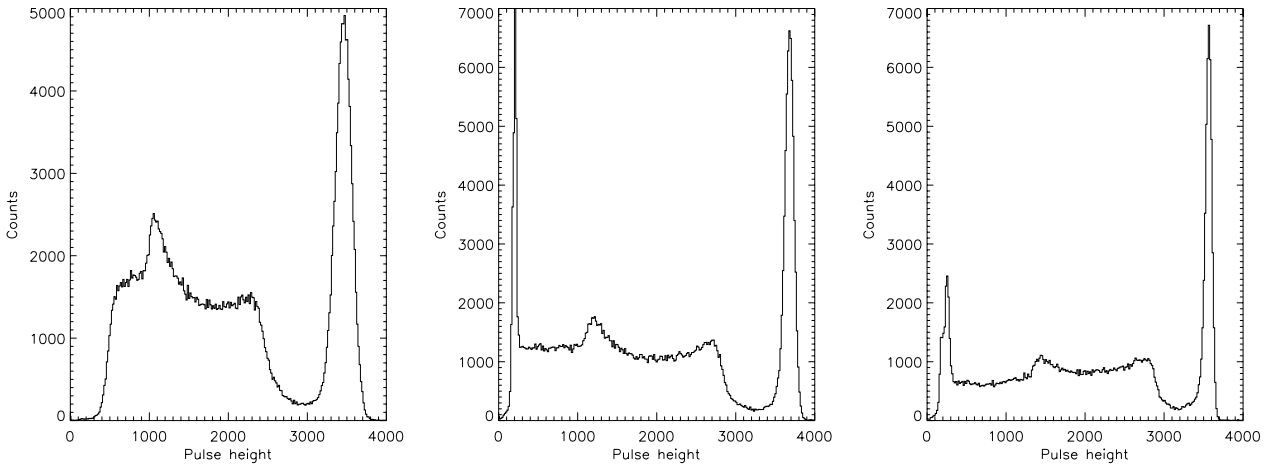

Figure 3. ^{137}Cs spectra measured for each scintillator directly coupled to a PMT. *Left:* NaI(Tl), with energy resolution of 7.5% FWHM. *Center:* $LaCl_3$, with energy resolution of 3.7%. *Right:* $LaBr_3$, with energy resolution of 2.8%.

coupled to the opposite end of the fibers with optical grease. The entire experimental setup was placed in a large light-tight box.

The data acquisition system consisted of a custom-built front-end electronics module feeding a 12-bit ADC (National Instruments PCI-6071E) with a trigger derived from the dynode signal of the energy PMT. The data acquisition software was written under LabVIEW 6.0. An uncollimated gamma-ray source was placed a few centimeters above the detector. Isotopes used included ^{137}Cs (662 keV), ^{22}Na (511 keV), ^{133}Ba (81, 276, 303, 356, and 384 keV), ^{57}Co (122 keV) and ^{241}Am (60 keV).

3. RESULTS

3.1. NaI

The left panel of Fig. 3 shows the ^{137}Cs spectrum measured in the NaI(Tl) detector directly coupled to the PMT. The energy resolution is 7.5% FWHM.

The spectra obtained with the fibers in place are shown in Figure 4. The energy resolutions measured in the energy PMT (measuring the light through the fibers) are 9.7% and 23% for ^{137}Cs and ^{57}Co respectively, while the energy resolutions measured in the fiber PMT (measuring the light trapped in the fibers) are 33% and 132%.

3.2. $LaCl_3$

The center panel of Fig. 3 shows the ^{137}Cs spectrum as measured in the $LaCl_3$ detector directly coupled to the PMT. The energy resolution is 3.7%. Measurements were made for gamma-ray energies ranging from 60 keV to 662 keV, with the pulse height varying linearly with energy to within 2% over the entire energy range.

The spectra obtained with the fibers in place are shown in Figure 5. The measured energy resolutions from the energy PMT are 9.5% and 31% for ^{137}Cs and ^{57}Co, respectively, while the energy resolutions measured in the fiber PMT are 20% and 59%.

3.3. $LaBr_3$

The right panel of Fig. 3 shows the ^{137}Cs spectrum measured in $LaBr_3$ directly coupled to the PMT. The energy resolution is 2.8%.

The spectra obtained with the fibers in place are shown in Figure 6. The measured energy resolutions from the energy PMT are 5.6% and 17% for ^{137}Cs and ^{57}Co, respectively, while the energy resolutions measured in the fiber PMT are 16% and 52%.

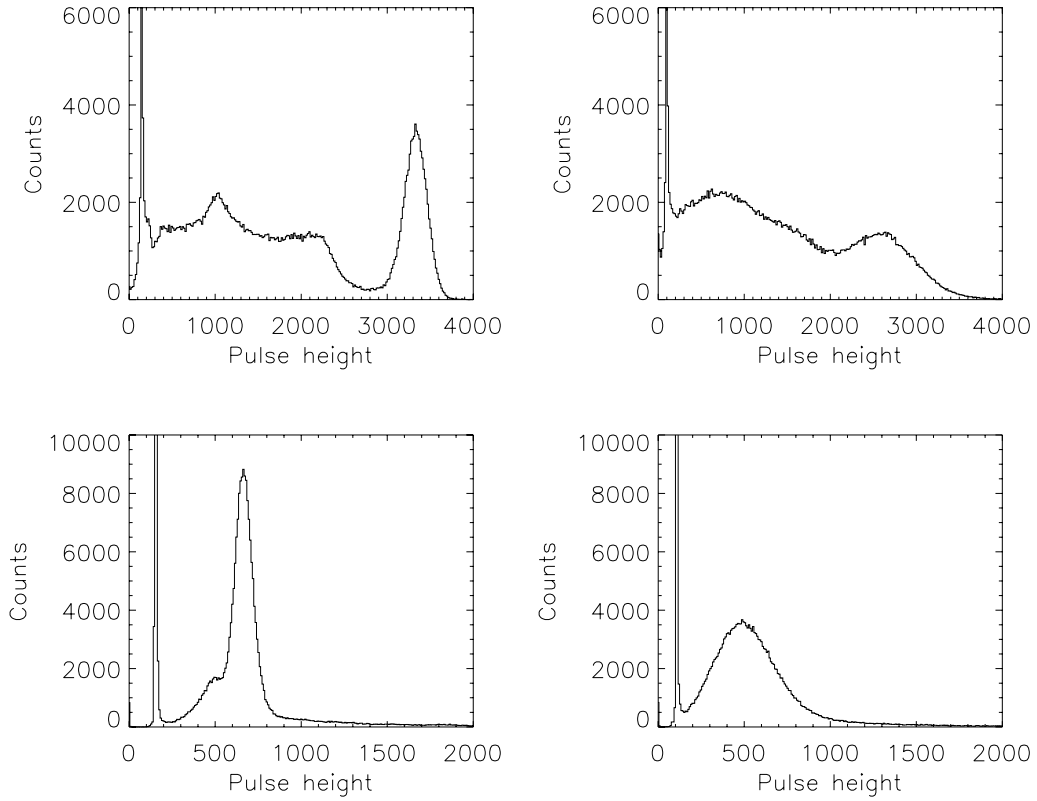

Figure 4. Spectra obtained from NaI(Tl) with WLS fibers in place. *Upper left:* ^{137}Cs spectrum measured in the energy PMT (resolution of 9.7%). *Upper right:* ^{137}Cs spectrum measured in the fiber PMT (resolution of 33%). *Lower left:* ^{57}Co spectrum measured in the energy PMT (resolution of 23%). *Lower right:* ^{57}Co spectrum measured in the fiber PMT (resolution of 132%).

4. DISCUSSION

As can be seen in Fig. 3, both the $LaCl_3$ and $LaBr_3$ crystals exhibit significantly better energy resolution than NaI(Tl), with $LaBr_3$ showing the best resolution of 2.8% FWHM at 662 keV. This is comparable to commercially available spectroscopy grade CZT ($\sim$ 3%; http://www.evproducts.com). Compared to CZT, $LaBr_3$ is much cheaper (and will likely get cheaper yet as demand increases) and has a much faster response time, enabling $LaBr_3$ to be used for timing and high count rate applications, without sacrificing performance.

The results with the WLS fibers in place (Figs. 4–6) demonstrate that the fibers provide a suitable match to the scintillators. While the energy resolution degrades when measured through the fibers, the resolution for the $LaBr_3$ measured with the energy PMT is still better than the resolution in the NaI(Tl) without the fibers. While $LaBr_3$ is currently more expensive than NaI(Tl), its better resolution along with higher density and faster decay time make it more suitable for high energy photon applications such as gamma-ray imaging. Since neither the BCF99-90 nor the BCF99-33A were optimized for their respective scintillator, it may be possible to tune the absorption band of the fibers to further increase the light yield in the fibers and improve the resolution and lower energy threshold measured with the fiber PMT.

The widths of the photopeaks as measured in the fiber PMT can be used to estimate the number of photoelectrons being produced by the WLS fibers. The width of the photopeak as determined by a Gaussian fit to the photopeak is assumed to be made up of contributions from counting statistics and noise, i.e. $\sigma_{\mathrm{T}}^2 = \sigma_{\mathrm{A}}^2 + \sigma_{\mathrm{B}}^2$,

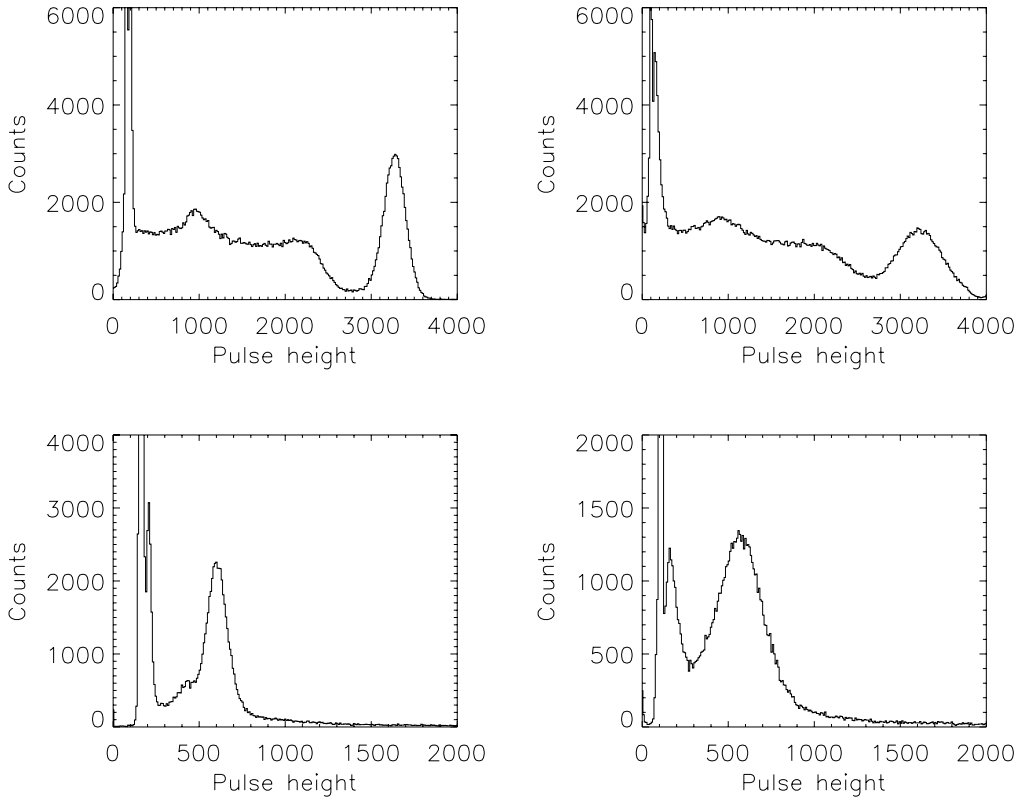

Figure 5. Spectra obtained from $LaCl_3$ with WLS fibers in place. *Upper left:* ^{137}Cs spectrum measured in the energy PMT (resolution of 9.5%). *Upper right:* ^{137}Cs spectrum measured in the fiber PMT (resolution of 20%). *Lower left:* ^{57}Co spectrum measured in the energy PMT (resolution of 31%). *Lower right:* ^{57}Co spectrum measured in the fiber PMT (resolution of 59%).

where σ_{T} is the measured width of the photopeak, σ_{A} is the statistical width, and σ_{B} is the width due to noise. The pulse height is linearly proportional to the number of photoelectrons, $A = kN$, where A is the fitted centroid of the photopeak and N is the number of photoelectrons. The resolution must be the same whether measured in units of pulse height or in units of photoelectrons, $\sigma_{\mathrm{A}}/A = \sigma_{\mathrm{N}}/N$. Then $\sigma_A = (A/N)\sigma_N = k\sqrt{N}$. Substituting into the original equation gives $\sigma_{\mathrm{T}}^2 = k^2N + \sigma_{\mathrm{B}}^2 = kA + \sigma_{\mathrm{B}}^2$. In other words, the square of the measured width is proportional to the pulse height. If a number of different gamma-ray energies are measured, then a linear fit to the square of the widths versus pulse height will give k. The number of photoelectrons contributing to a given photopeak is then $N = A/k$.

Measurements were made using gamma-ray energies ranging from 60 to 662 keV and a linear fit made to the square of the photopeak widths versus pulse height. The number of photoelectrons were then calculated for the sum of the 12 fibers. Table 3 lists the number of photoelectrons calculated from the ^{57}Co source with a gamma-ray energy of 122 keV.

Since the photoelectron numbers given in Table 3 are the values measured in the sum of all 12 fibers, the effective energy threshold cannot be determined directly from these measurements. This is because 1) the individual fibers presented varying exposures to scintillation light produced by the uncollimated source at different locations in the crystal due to the depth of the detector relative to the lateral dimensions, and 2) even for a single photon, the distribution of light across the fibers was not uniform due to the circular optical window. A proper determination of energy threshold will require a measurement of the light from individual fibers, e.g.

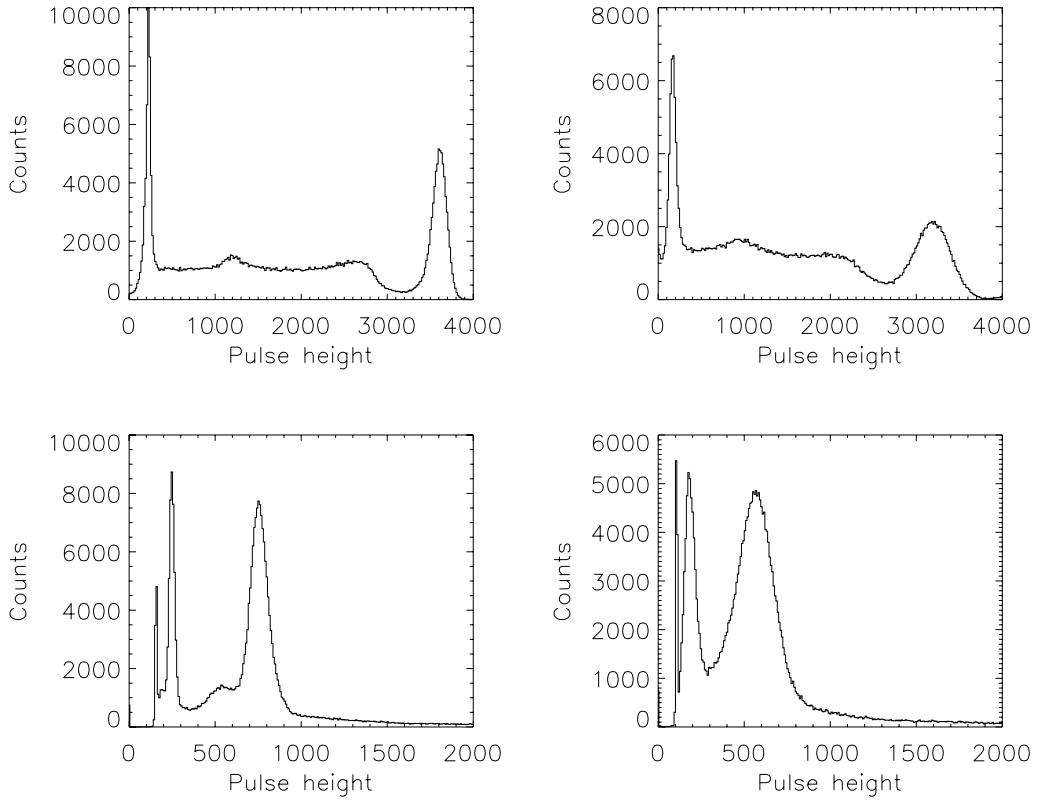

Figure 6. Spectra obtained from $LaBr_3$ with WLS fibers in place. *Upper left:* ^{137}Cs spectrum measured in the energy PMT (resolution of 5.6%). *Upper right:* ^{137}Cs spectrum measured in the fiber PMT (resolution of 16%). *Lower left:* ^{57}Co spectrum measured in the energy PMT (resolution of 17%). *Lower right:* ^{57}Co spectrum measured in the fiber PMT (resolution of 52%).

using a multi-anode PMT. These measurements (together with comparisons with Monte Carlo simulations of the photon propagation in the scintillator/fiber geometry) are planned for the near future in order to determine the energy threshold and position resolution in detail. Nevertheless, dividing the total measured photoelectron counts in Table 3 by 12 fibers ought to provide a lower limit for the number of photoelectrons in the central fiber. The measured $LaBr_3$ result (> 3 photoelectrons per fiber at 122 keV) suggests that the approach holds promise.

Table 3. Integrated number of photoelectrons detected in all 12 WLS fibers for ^{57}Co (122 keV).

Detector	Fiber	Number of PE
NaI(Tl)	Washington Univ.	8
$LaCl_3$	BCF99-90	23
$LaBr_3$	BCF99-33A	37

5. CONCLUSION

Measurements were made using NaI(Tl), $LaCl_3$, and $LaBr_3$ both with and without wavelength shifting fibers. The energy resolutions of the lanthanum halides were better than that of NaI(Tl) in all cases, with $LaBr_3$ being significantly better. While the detector geometry was not optimal for determining the minimum energy threshold in the fibers, the lower limit derived here of > 3 photoelectrons per fiber at 122 keV shows the promise of the crossed fiber imager approach when combined with $LaBr_3$.

A gamma-ray imager based on a scintillator with WLS crossed fiber readout is being considered for the Coded Aperture Survey Telescope for Energetic Radiation (CASTER) instrument being studied for NASA's Black Hole Finder Probe mission.[4,5] CASTER is an imaging hard x-ray/low energy gamma-ray instrument with a baseline energy range of $10 - 600$ keV, minute-of-arc angular resolution, and a wide field-of-view. In order to approach 600 keV, a detector thickness ~ 1 cm is required with a detector area in excess of 1 m^2. $LaBr_3$ and $LaCl_3$ offer the capability of providing the desired energy resolution and sensitivity at high energies at a lower cost than that of CZT. At energies down to ~ 100 keV, the fiber readout approach with $LaBr_3$ appears to provide enough light in 2 mm fibers to give position resolution sufficient for minute-of-arc angular resolution coded aperture imaging with a mask at a distance of ~ 1.5 m and mask elements $\sim 5 - 10$ mm. For lower energies, an array of segmented lanthanum halide detectors fabricated as optically isolated 2 mm $\times$ 2 mm pixels concentrates the majority of the scintillation light into a single fiber rather than allowing it to expand in an isotropic light sphere that illuminates multiple fibers, and should allow the threshold to be lowered significantly. Test results with segmented scintillators will be reported separately.

The combination of lanthanum halide scintillator and crossed fiber imager is also applicable as a monitoring device for detecting contraband nuclear material. We are currently constructing a prototype instrument (High Sensitivity Gamma Ray Imager, HISGRI) suitable for detecting radioactive cargoes on ships entering a harbor. On the assumption that such a shipment would be heavily shielded, the emphasis in the HISGRI design is placed on obtaining the highest sensitivity possible in order to detect a shipment of shielded radionuclides (i.e., " dirty bomb " material) at large distances. For the radionuclide detection application, an energy threshold of 100 keV is perfectly suitable, and we are proceeding to construct a prototype coded aperture imager based on $LaBr_3$ scintillator read out with BCF99-33A wave-shifting fibers as described here.

Future plans include utilizing detectors with a geometry more appropriate for testing the performance of the WLS crossed fiber read out. This will include square detectors with optical windows on both sides as well as pixelated detectors. Orthogonal layers of WLS fibers will be coupled to these detectors and the individual fibers read out with a multi-anode PMT. This will allow us to measure the energy threshold of the individual fibers and characterize the position resolution and minimum energy threshold in detail.

ACKNOWLEDGMENTS

We wish to thank C. Dathy, M. Kushner, C. Rozsa, and their colleagues at St. Gobain Crystals and Detectors for providing the $LaCl_3$ and $LaBr_3$ detectors and R. Binns and P. Dowkontt at Washington University for providing the WLS fibers for the NaI detector. This work was supported in part by US Dept. of Energy NNSA Cooperative Agreement DE-FC52-04-NA25683.

REFERENCES

1. E. V. D. van Loef, P. Dorenbos, C. W. E. van Eijk, K. W. Kramer, and H. J. Gudel, "High energy resolution scintillator: Ce^{3+} activated $LaCl_3$," *Appl. Phys. Lett.* **77**, pp. 1467–1468, 2000.
2. E. V. D. van Loef, P. Dorenbos, C. W. E. van Eijk, K. W. Kramer, and H. J. Gudel, "High energy resolution scintillator: Ce^{3+} activated $LaBr_3$," *Appl. Phys. Lett.* **79**, pp. 1573–1575, 2001.
3. http://www.bicron.com, St. Gobain Crystals and Detectors, Newbury, OH.
4. M. L. McConnell *et al.*, "CASTER - a scintillator-based Black Hole Finder Probe," *Proc. SPIE* **5488**, in press, 2004.
5. M. L. McConnell *et al.*, "CASTER - a concept for a Black Hole Finder Probe based on the use of new scintillator technology," *Proc. SPIE* **5898**, these proceedings, 2005.